NASA/TP—2011–216457

The Effects of Foam Thermal Protection System on the Damage Tolerance Characteristics of Composite Sandwich Structures for Launch Vehicles

A.T. Nettles, A.J. Hodge, and J.R. Jackson
Marshall Space Flight Center, Marshall Space Flight Center, Alabama

February 2011

The NASA STI Program…in Profile

Since its founding, NASA has been dedicated to the advancement of aeronautics and space science. The NASA Scientific and Technical Information (STI) Program Office plays a key part in helping NASA maintain this important role.

The NASA STI Program Office is operated by Langley Research Center, the lead center for NASA's scientific and technical information. The NASA STI Program Office provides access to the NASA STI Database, the largest collection of aeronautical and space science STI in the world. The Program Office is also NASA's institutional mechanism for disseminating the results of its research and development activities. These results are published by NASA in the NASA STI Report Series, which includes the following report types:

- TECHNICAL PUBLICATION. Reports of completed research or a major significant phase of research that present the results of NASA programs and include extensive data or theoretical analysis. Includes compilations of significant scientific and technical data and information deemed to be of continuing reference value. NASA's counterpart of peer-reviewed formal professional papers but has less stringent limitations on manuscript length and extent of graphic presentations.

- TECHNICAL MEMORANDUM. Scientific and technical findings that are preliminary or of specialized interest, e.g., quick release reports, working papers, and bibliographies that contain minimal annotation. Does not contain extensive analysis.

- CONTRACTOR REPORT. Scientific and technical findings by NASA-sponsored contractors and grantees.

- CONFERENCE PUBLICATION. Collected papers from scientific and technical conferences, symposia, seminars, or other meetings sponsored or cosponsored by NASA.

- SPECIAL PUBLICATION. Scientific, technical, or historical information from NASA programs, projects, and mission, often concerned with subjects having substantial public interest.

- TECHNICAL TRANSLATION. English-language translations of foreign scientific and technical material pertinent to NASA's mission.

Specialized services that complement the STI Program Office's diverse offerings include creating custom thesauri, building customized databases, organizing and publishing research results…even providing videos.

For more information about the NASA STI Program Office, see the following:

- Access the NASA STI program home page at <http://www.sti.nasa.gov>

- E-mail your question via the Internet to <help@sti.nasa.gov>

- Fax your question to the NASA STI Help Desk at 443–757–5803

- Phone the NASA STI Help Desk at 443–757–5802

- Write to:
  NASA STI Help Desk
  NASA Center for AeroSpace Information
  7115 Standard Drive
  Hanover, MD 21076–1320

NASA/TP—2011–216457

The Effects of Foam Thermal Protection System on the Damage Tolerance Characteristics of Composite Sandwich Structures for Launch Vehicles

A.T. Nettles, A.J. Hodge, and J.R. Jackson
Marshall Space Flight Center, Marshall Space Flight Center, Alabama

National Aeronautics and
Space Administration

Marshall Space Flight Center • MSFC, Alabama 35812

February 2011

Available from:

NASA Center for AeroSpace Information
7115 Standard Drive
Hanover, MD 21076–1320
443–757–5802

This report is also available in electronic form at
<https://www2.sti.nasa.gov>

TABLE OF CONTENTS

LIST OF FIGURES

LIST OF FIGURES (Continued)

LIST OF TABLES

LIST OF ACRONYMS AND SYMBOLS

Al	aluminum
BVID	barely visible impact damage
CAI	compression-after-impact
IFF	interfiber failure
IRT	infrared thermography
NDE	nondestructive evaluation
TPS	thermal protection system
UHMWPE	ultrahigh-molecular-weight polyethelene

TECHNICAL PUBLICATION

THE EFFECTS OF FOAM THERMAL PROTECTION SYSTEM ON THE DAMAGE TOLERANCE CHARACTERISTICS OF COMPOSITE SANDWICH STRUCTURES FOR LAUNCH VEHICLES

1. INTRODUCTION

A satisfactory demonstration of damage tolerance is required as part of a risk reduction program for using composite components on future manned launch vehicles.[1] The vast majority of past studies on the foreign object impact damage characteristics of composite laminates have been on bare components where the impacting object came in direct contact with the outer ply of the laminate; however, many launch vehicle components are covered with a thermal protection system (TPS) to meet thermal requirements during flight. Since the TPS will be in place for the majority of the component's life, especially when it is most vulnerable to foreign object impacts (transportation and assembly), the effect of impact damage to the composite laminate with the TPS is needed since the impact characteristics can change due to the presence of the TPS.

In a European study of the effects of a cork TPS for launch vehicle fairing applications, the damage morphology and resulting residual strength of the composite laminate were heavily influenced by the presence of cork TPS.[2] It was noted that the TPS acted as a very good visual indicator of an impact damage event and delayed the impact energy at which damage formed in the composite laminate. At higher impact levels, the TPS caused a larger damage zone compared to bare laminates due to the load spreading effect of the cork; however, the compression-after-impact (CAI) strength was consistently higher for the TPS covered laminates when based on impact energy or damage size as detected by C-scan. Two findings of note in the cork covered laminates are: (1) Impact damage morphology is different with less matrix cracking and fewer but longer delaminations and (2) some impacted specimens had reduced compression strength even with no detectable damage from the C-scan.

Other studies have examined the impact damage characteristics of carbon/epoxy laminates covered with other materials, not for thermal requirements but to enhance the damage tolerance characteristics of the laminate. Ultra-high-molecular-weight polyethylene (UHMWPE) was placed on one or both outer surfaces of carbon/epoxy laminates to enhance damage tolerance characteristics in at least four studies.[3–6]

In reference 3, it was found that as the amount of UHMWPE fiber increased so did the amount of impact energy absorbed by the specimen, as measured by instrumented impact tests. These data were for carbon/epoxy laminates with the top one-fourth or two-fifths of the laminate made of UHMWPE.

Reference 4 examined the CAI strength of impact damaged eight-ply laminates that consisted of the following three types of specimens: (1) All eight plies being carbon, (2) one outer ply on each side having UHMWPE fiber replace the carbon fiber, and (3) the outer two plies on each side having UHMWPE fiber replace the carbon fiber. The damage area as measured by ultrasonic C-scan showed that at high-impact energy (12 J) the specimen with two layers of UHMWPE on front and back had larger damage areas compared to the all carbon and one-ply UHMWPE specimens. However, when tested for CAI strength, the specimens with the outer two plies having UHMWPE had higher normalized CAI strengths despite the larger damage area. If the UHMWPE was placed on only one side of the specimen, a greater CAI strength was seen when the UHMWPE was on the back (nonimpacted) side of the laminate. The same results were found in reference 5 for residual flexural strength although the damage area decreased with additional outer plies of UHMWPE at all impact energy levels tested.

Reference 6 tested both honeycomb sandwich panels and monolithic laminates with one layer of UHMWPE at various locations. Instrumented impact data showed little difference except for the honeycomb samples (which had a higher maximum load of impact once fibers were broken); at which point, the specimens with UHMWPE could withstand higher loads due to the delay of fiber breakage onset. For honeycomb specimens, cross-sectional examination of the impact damage zone showed that the specimens without UHMWPE contained more through-thickness damage than specimens with a layer of UHMWPE, although C-scan images showed little difference in damage area. The CAI results showed no difference in specimens with and without UHMWPE. It was noted that the most beneficial aspect of the UHMWPE was that it acted as a good impact indicator as a distinct white spot was made on the UHMWPE.

Prior research demonstrates that covering a laminate with another layer of material generally causes larger damage areas as detected by nondestructive evaluation (NDE), but CAI strength is unaffected or improved due to the different damage morphology within the impacted laminate.

In an effort to protect composite laminates from impact damage, a few studies were examined using a structure bonded to a composite laminate.[7,8] In reference 7, core material (honeycomb or Rohacell foam) with an outer face sheet consisting of three plies of various fiber/resin systems was assessed for both damage protection and damage detection with favorable results. In reference 8, a surface layer of low-density adhesive filled with glass microballoons covered with three layers of aluminum (Al) gauze was found to protect the composite laminate and act as an improved visual aid for impact damage.

The protection of composite (and metallic) aircraft parts has not gone unnoted, as there are at least two commercial products available to protect surfaces from impact. These consist of applying adhesive sheets with coatings of polyester/polyethylene[9] or polyurethane[10] to surfaces that require impact protection.

Although these applications are specifically designed to enhance damage tolerance characteristics,[3–10] the results of these studies may be applicable to the damage tolerance characteristics of a laminated composite structure with a TPS coating. Since it has been demonstrated that the amount and type of damage can be influenced by a surface coating/covering, the impact response of a carbon/epoxy sandwich structure covered with foam TPS (identical to that planned to be used on the Ares I interstage) was the aim of this study.

2. MATERIALS

The TPS utilized in this study is sprayable polyurethane foam planned for use on the Ares I composite interstage. The foam has a nominal thickness of about 0.3 in with a variation of ±0.05 in. The areal density of the foam is 0.06 lb/ft^2. The surface of the foam itself is not smooth but of a coarse texture as shown in figure 1.

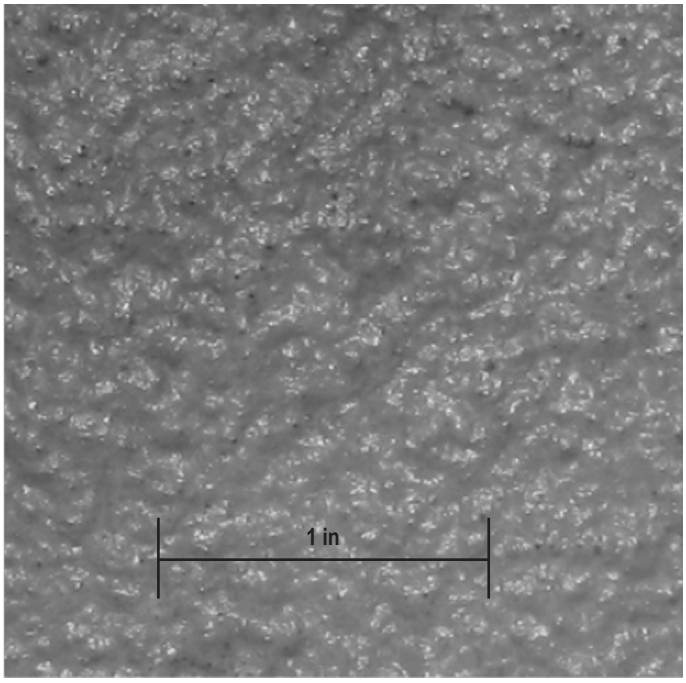

Figure 1. Surface texture of TPS foam used in this study.

The foam-covered composite consists of a sandwich structure planned for use on the Ares I composite interstage. This sandwich structure has 18-ply face sheets and an Al honeycomb core. An Al screen (to serve as a lightning strike protection) is applied to the outer surface of the sandwich structure with epoxy film adhesive before the TPS foam is applied. This screen is nominally 0.005 in thick and has approximately 12 meshes per inch. The areal density of the Al screen is 0.016 lb/ft^2. The core used is perforated 5052 Al honeycomb with 0.125-in cell size having a density of 3.1 lb/ft^3 and thickness of 1 in, which gives an areal density of 0.26 lb/ft^2. The face sheets consist of IM7/8552 carbon/epoxy and the film adhesive used to bond the face sheet to the core was FM-300K having an areal density of 0.08 lb/ft^2. The layup of the 18-ply face sheets was [+45,0,–45,0,90,0,0,90,0]S.

Each carbon/epoxy face sheet had a thickness of 0.115 in, an areal density of 0.94 lb/ft^2, and was cocured to the honeycomb core. The honeycomb sandwich panels were manufactured as 24- × 24-in square sandwich plates from which, 4- × 6-in specimens were machined for impact and subsequent compression testing. This gave each specimen a structural load bearing (laminate) cross-sectional area of 0.92 in^2, which was used to calculate the breaking stresses. Testing of the lightning strike layer showed that it has compression strength of about 20.6 ksi and a compression modulus of 0.68 Msi. The strength is 42% less than the lamina transverse compression strength of the material used for the laminate, and the modulus is 53% lower than the modulus of a transverse ply. For an undamaged 18-ply laminate with 10 plies at 0°, the contribution to strength of the lightning strike layer should be negligible.

A schematic of the cross section of the sandwich structure with TPS is shown in figure 2.

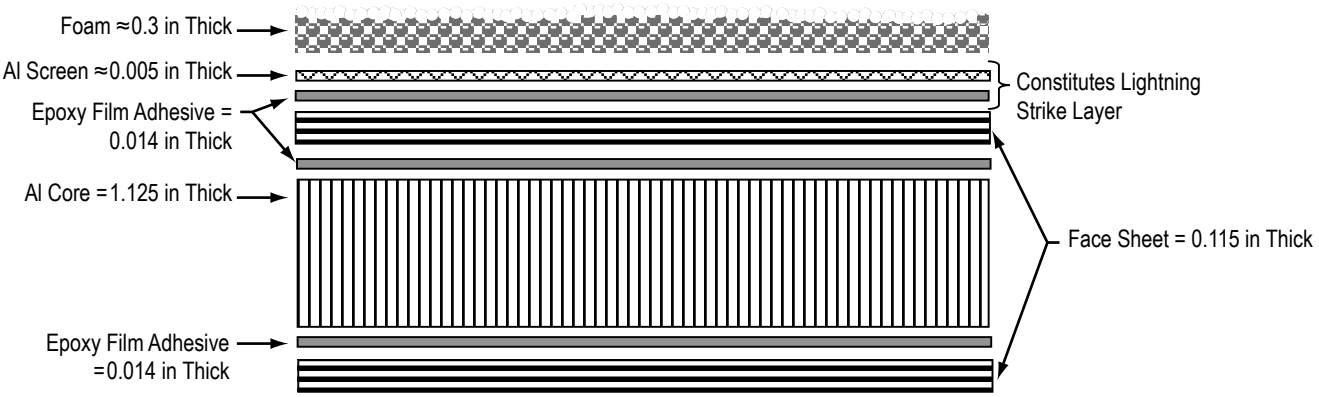

Figure 2. Sandwich structure used in this study.

In order to decouple the impact response of the lightning strike layer and foam TPS, some specimens had the TPS removed before impact with only the lightning strike layer covering the sandwich specimen.

In addition to the specimens with the lightning strike layer (screen) and TPS on the outer surface of the sandwich structure, baseline specimens with no screen or TPS were also tested in this study. This gave a total of three types of specimens used in this study: (1) Bare—those with no covering, (2) screen—those covered only with the lightning screen and film adhesive, and (3) foam—those with both the lightning strike layer and foam TPS covering the face sheets.

The areal density of the bare, screen, and foam specimens is 2.3 lb/ft^2, 2.4 lb/ft^2, and 2.46 lb/ft^2, respectively, representing a mass increase of 4.3% for the screen specimens and 6.9% for the foam specimens over the bare specimens. Undamaged specimens tested in compression gave an average strength of 75.8 ± 2.4 ksi. The presence of the lightning strike mesh had no effect on the virgin compression strength.

3. EXPERIMENTAL

3.1 Impact Testing

A drop-weight tower was used to impact the sandwich specimens with a range of impact energies. The height of the dropped weight was adjusted to vary the impact energy. A hemispherical impactor (tup) with a diameter of 0.5 in was used throughout this study. The amount of weight used was 2.7 lb. The velocity of the falling weight was measured just prior to impact to calculate an impact energy since some of the speed of the falling weight was lost due to friction with the guideposts, and the simple weight × height formula could not be used with accuracy.

3.2 Visual Examination

Damage due to impact was documented with digital photography of the surface. TPS-coated specimens then had the foam removed and additional photographs were acquired to compare surface damage between the coated and uncoated specimens.

3.3 Nondestructive Examination Testing

The damage in the specimens was assessed with infrared thermography (IRT). IRT is an NDE technique that uses a sensitive infrared camera to monitor heat dissipation from a surface induced with a flash of heat from a quartz lamp. Any areas of damage will dissipate heat at a different rate than undamaged material and the results seen are termed 'indications.' A typical indication for the type of specimen used in this study is shown in figure 3. This two-dimensional indication assesses the planar area of damage within the specimen. In a previous study,[11] damage width (damage size perpendicular to the loading direction) was shown to be the best indicator of residual strength, thus this parameter was used in this study. The foam covered specimens had the foam removed before IRT evaluation.

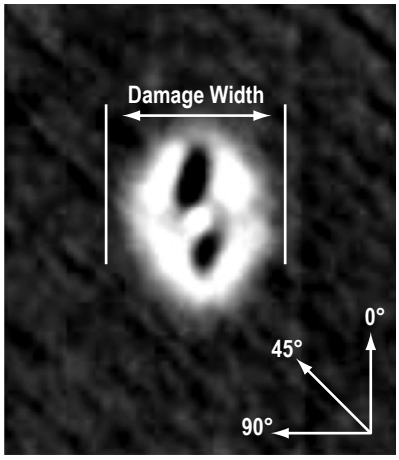

Figure 3. Typical IRT indication of impact damaged laminate.

3.4 Cross-Sectional Microscopy

Honeycomb sandwich panels representing the three types of specimens (bare, screen, and foam) examined in this study were impacted at a wide range of energy levels and then cross-sectioned to ascertain the differences in trough-thickness damage morphology. The specimens were sectioned in the 0° direction through the center of the impact zone. The sectioned specimens were then polished (on the cut side) with successively finer grit silicon carbide paper on a polishing wheel. Once polished, the cross sections were examined under an optical microscope.

3.5 Compression-After-Impact Testing

Specimens of the bare, screen, and foam configurations that measured 4×6 in were tested for residual compression strength after impact. The specimens were prepared for compression testing once they had been impacted, photographed, and the foam TPS removed (if initially present). The ends of the specimens were potted into Al frames and then machined flat and parallel to within ±0.001-in tolerance. Details of the specimen and testing procedure can be found in reference 11.

4. RESULTS

4.1 Damage Width

Comparisons of the IRT indications for the three types of specimens examined in this study are shown in figure 4.

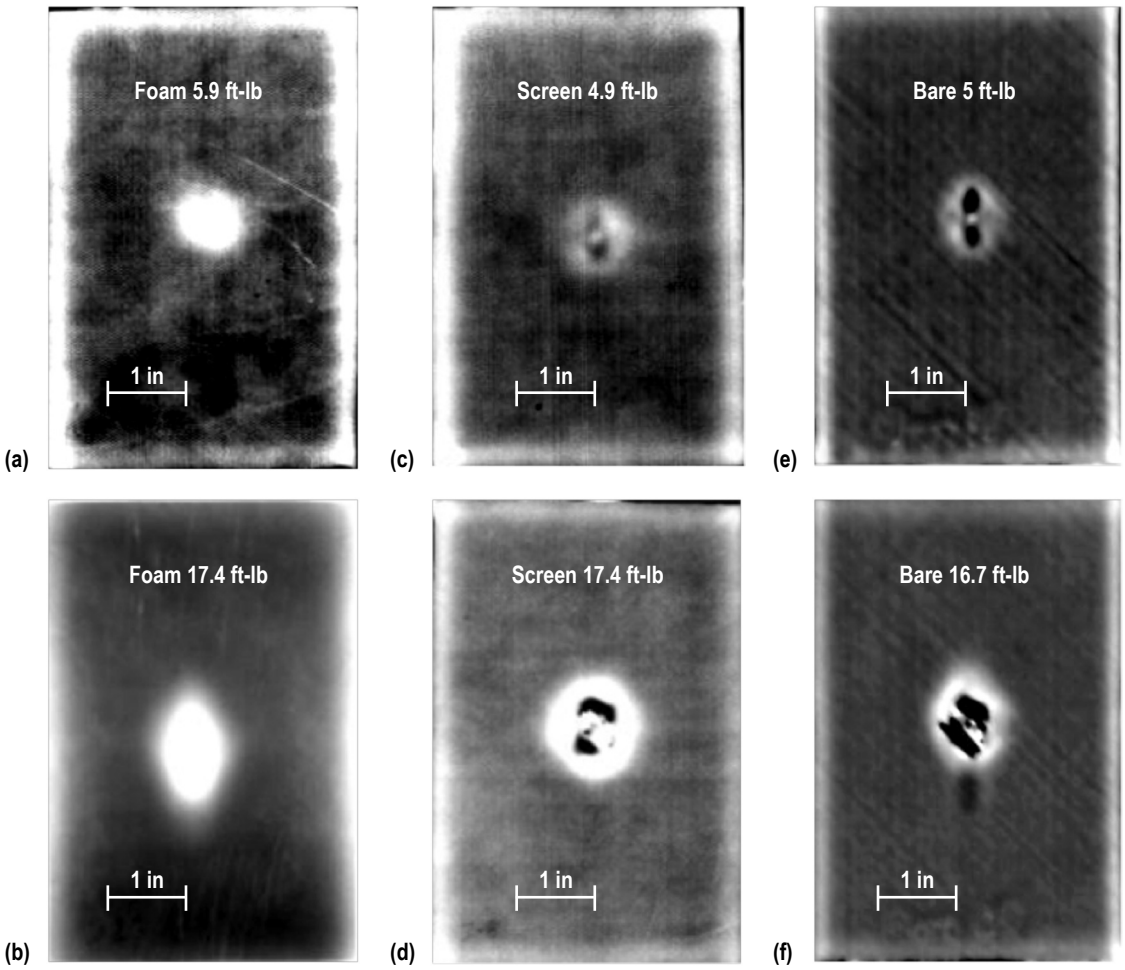

Figure 4. Comparison of IRT results for foam covered ((a) and (b)), screen ((c) and (d)), and bare ((e) and (f)) specimens at low ((a), (c), and (e)) and high ((b), (d), and (f)) impact energies.

Differences in damage geometry were observed in the IRT results. At high-impact energies, the indication on the foam-covered specimen is more elliptical compared to the more circular indications on the bare and screen specimens.

Results from the impact tests on bare, screen, and foam specimens are plotted in figure 5 for damage width as detected by NDE. The data are presented in table 1.

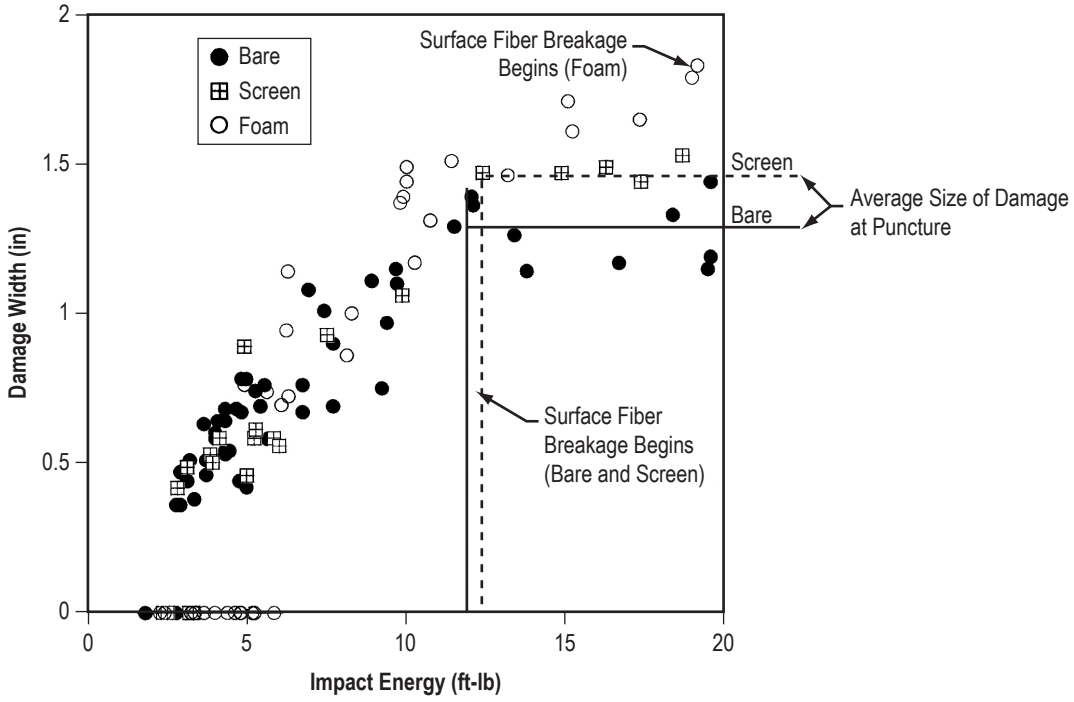

Figure 5. NDE width from table 1.

From the plot in figure 5, it appears that the TPS has little effect on the damage width formed at low-impact energies (up to ≈10 ft-lb in this case). However, at higher impact energies, the screen and foam specimens show a larger damage width for a given impact energy. The bare and screen specimens exhibited surface fiber breakage at ≈12 ft-lb, indicating the start of complete puncture of the impacted face sheet. The foam specimens did not show the onset of puncture until about 19 ft-lb, which was the upper limit used in this study.

Typically, when damage size is plotted as a function of impact energy, the size increases with increasing impact energy until the start of puncture. At this energy and above, the size remains fairly constant as a hole is formed in the laminate by the impactor.[12] This effort found that this constant size at penetration is 16% higher for the screen specimens than for the bare specimens, probably due to the extra layer acting as a load spreader, as it did in references 2 and 4–6. The foam layer required 58% greater impact energy to achieve puncture. It is anticipated that further measurements of damage size for impacts greater than 19 ft-lb would not increase the average damage size. Therefore, the TPS foam-covered specimens delayed the onset of visible fiber breakage in the outer plies.

Table 1. Results from impact tests on baseline (bare), lightning protection (screen), and thermal protection (foam) specimens.

Bare Specimen I.D.	Impact Energy (ft-lb)	NDE Size (in)	Screen Specimen I.D.	Impact Energy (ft-lb)	NDE Size (in)	Foam Specimen I.D.	Impact Energy (ft-lb)	NDE Size (in)
Bare-1	4.3	0.53	Screen-1	18.7	1.53	Foam-1	11.4	1.51
Bare-2	4.3	0.68	Screen-2	17.4	1.44	Foam-2	3.3	0
Bare-3	4.8	0.67	Screen-3	16.3	1.49	Foam-3	2.2	0
Bare-4	4.8	0.78	Screen-4	14.9	1.47	Foam-4	4.9	0.76
Bare-5	5.5	0.76	Screen-5	12.4	1.47	Foam-5	6.3	1.14
Bare-6	5.4	0.69	Screen-6	9.9	1.06	Foam-6	2.4	0
Bare-7	13.4	1.26	Screen-7	7.5	0.93	Foam-7	15.1	1.71
Bare-8	13.8	1.14	Screen-8	4.9	0.89	Foam-8	9.9	1.39
Bare-9	9.7	1.10	Screen-9	2.5	0	Foam-9	10.0	1.49
Bare-10	11.5	1.29	Screen-10	2.3	0	Foam-10	10.0	1.44
Bare-11	12.1	1.36	Screen-11	2.5	0	Foam-11	8.26	1.00
Bare-12	8.9	1.11	Screen-12	2.8	0.42	Foam-12	8.12	0.86
Bare-13	7.4	1.01	Screen-13	3.2	0	Foam-13	10.3	1.17
Bare-14	6.9	1.08	Screen-14	3.1	0.49	Foam-14	10.7	1.31
Bare-15	1.8	0	Screen-15	3.3	0	Foam-15	9.8	1.37
Bare-16	1.8	0	Screen-16	3.8	0.53	Foam-16	13.2	1.46
Bare-17	1.8	0	Screen-17	3.9	0.50	Foam-17	17.4	1.65
Bare-18	2.7	0	Screen-18	4.1	0.58	Foam-18	19.0	1.79
Bare-19	2.7	0.36	Screen-19	5.0	0.46	Foam-19	19.2	1.83
Bare-20	4.3	0.54	Screen-20	5.2	0.58	Foam-20	15.2	1.61
Bare-21	6.7	0.76	Screen-21	5.8	0.58	Foam-21	3.2	0
Bare-22	6.7	0.67	Screen-22	6.0	0.56	Foam-22	3.6	0
Bare-23	2.9	0.36	Screen-23	5.3	0.61	Foam-23	4.0	0
Bare-24	2.9	0.47				Foam-24	4.4	0
Bare-25	3.1	0.44				Foam-25	4.6	0
Bare-26	9.7	1.15				Foam-26	4.8	0
Bare-27	12.0	1.39				Foam-27	4.8	0
Bare-28	16.7	1.17				Foam-28	5.2	0
Bare-29	20.4	1.32				Foam-29	5.1	0
Bare-30	19.6	1.15				Foam-30	5.6	0.74
Bare-31	19.6	1.44				Foam-31	5.8	0
Bare-32	19.6	1.19				Foam-32	6.2	0.94
Bare-33	18.4	1.33				Foam-33	6.3	0.72
Bare-34	7.7	0.69				Foam-34	6.1	0.69
Bare-35	7.7	0.90						
Bare-36	9.2	0.75						
Bare-37	9.4	0.97						
Bare-38	4.4	0.54						
Bare-39	4.7	0.44						
Bare-40	4.9	0.42						
Bare-41	5.6	0.58						
Bare-42	3.6	0.63						
Bare-43	4.1	0.64						
Bare-44	4.3	0.64						
Bare-45	4.6	0.68						
Bare-46	4.9	0.78						
Bare-47	5.2	0.74						
Bare-48	3.1	0.44						
Bare-49	3.3	0.38						
Bare-50	3.2	0.51						
Bare-51	3.7	0.46						
Bare-52	3.7	0.51						
Bare-53	4.0	0.58						
Bare-54	4.0	0.60						

Examining the data at low-impact energies shows that the foam appears to delay the onset of when any detectable damage from IRT testing begins to form. The data in table 1 are plotted in figure 6 at low-impact energies to better illustrate this effect.

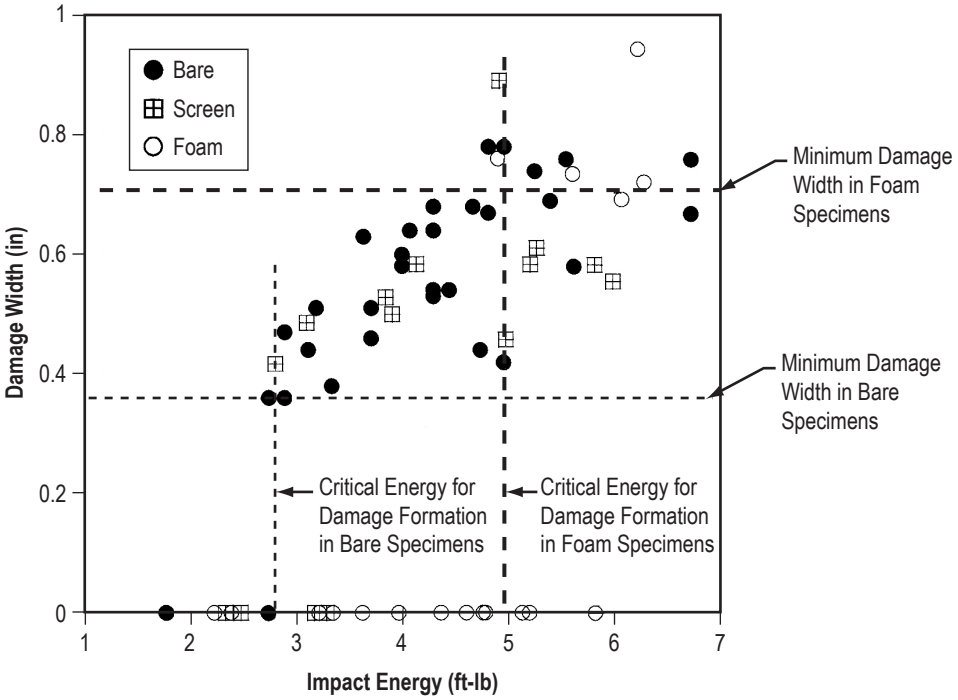

Figure 6. NDE width from table 1 at low impact energies.

The bare specimens do not demonstrate damage as detected by NDE until about 2.8 ft-lb. Once detectable damage does appear, it has a minimum value of about 0.37 in. The specimens covered with the lightning strike layer (screen) differ little from the bare specimens. The foam-covered specimens do not demonstrate detectable damage until about 5 ft-lb of impact energy. Once detectable damage does appear in the foam-covered specimens, it has a minimum width of about 0.7 in. Therefore, the critical energy at which detectable impact damage forms is 79% greater for the foam-covered specimens than for the bare or screen-covered specimens. The minimum detectable damage size that forms is 89% greater for the foam specimens than for the bare or screen specimens. At the lower range of impact energies, the foam layer has a more pronounced effect on the sandwich specimens than the lightning strike layer. At the higher range of impact energies used in this study, both layers contribute to give a larger IRT damage size than for the bare specimens.

It is recommended that residual strength testing be performed even when damage is not detected when determining the effect of low-velocity impact on coated or protected laminates, as small damage may still result in reductions to compression strength as found in reference 2. In this study, where the specimens indicated no damage was present, no drop in compressive strength was demonstrated.

4.2 Visual Examination

Examples of the visual damage on foam, screen, and bare specimens are shown in figure 7 for very low-impact energies. The TPS acts as a good impact indicator since the impact was clearly visible on the specimens covered with foam, whereas there was no visible damage on the screen or bare specimens. Barely visible impact damage (BVID) on the screen-covered specimens was not evident until impact energy of 12.4 ft-lb was reached. For the bare specimens, BVID was evident at the 8.5-ft-lb impact energy level. It should be noted that BVID requires a specific definition for any given structure and is dependent upon many variables including examiner, lighting, surface finish, proximity to impact site, etc. It is not the intent of this study to define BVID. However, photographs are included in figure 8 to give the reader a better assessment of the type of damage considered BVID in this particular study.

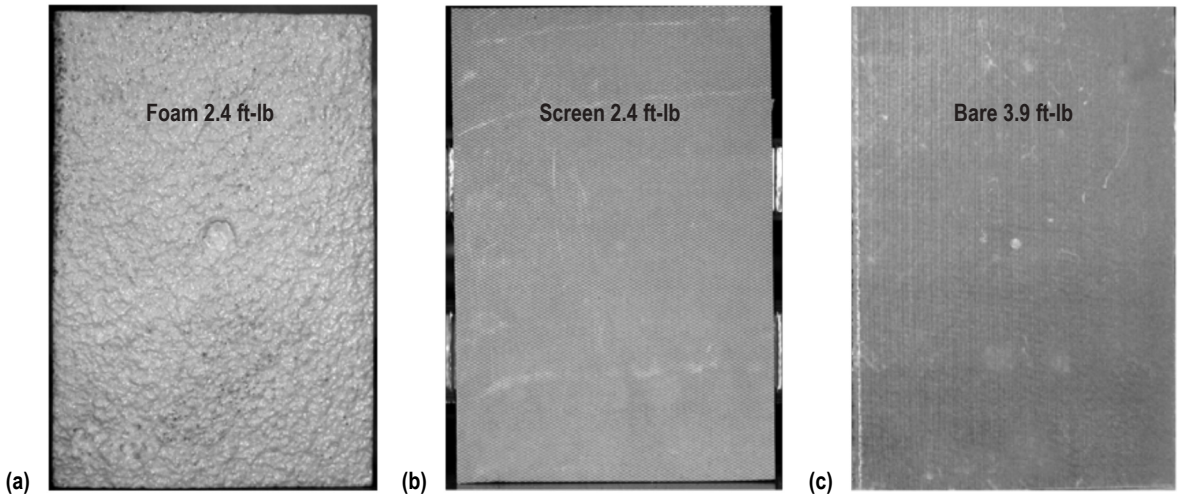

Figure 7. Visual damage of TPS and screen specimens ((a) and (b)) impacted at 2.4 ft-lb and a bare specimen (c) impacted at 3.9 ft-lb.

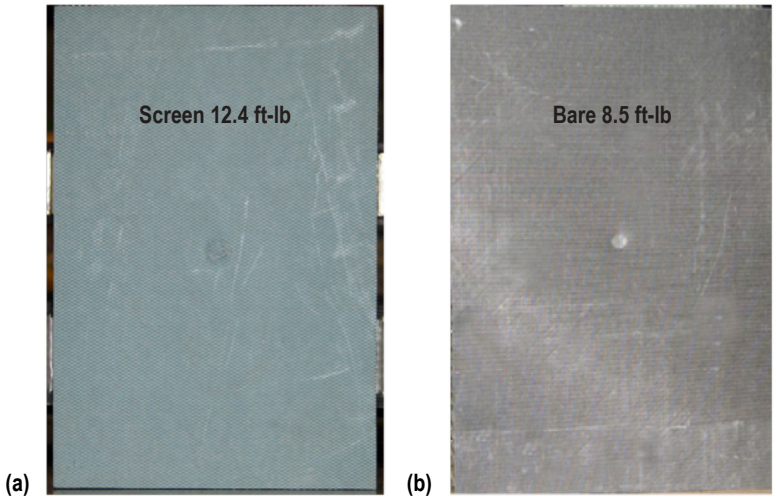

Figure 8. Examples of the onset of BVID for (a) screen and (b) bare.

For the foam-covered specimens, the foam was removed from the impacted specimens to ascertain the extent of visual damage beneath the foam. Examples of the three specimen types examined in this study that were impacted at high-impact levels are shown in figure 9.

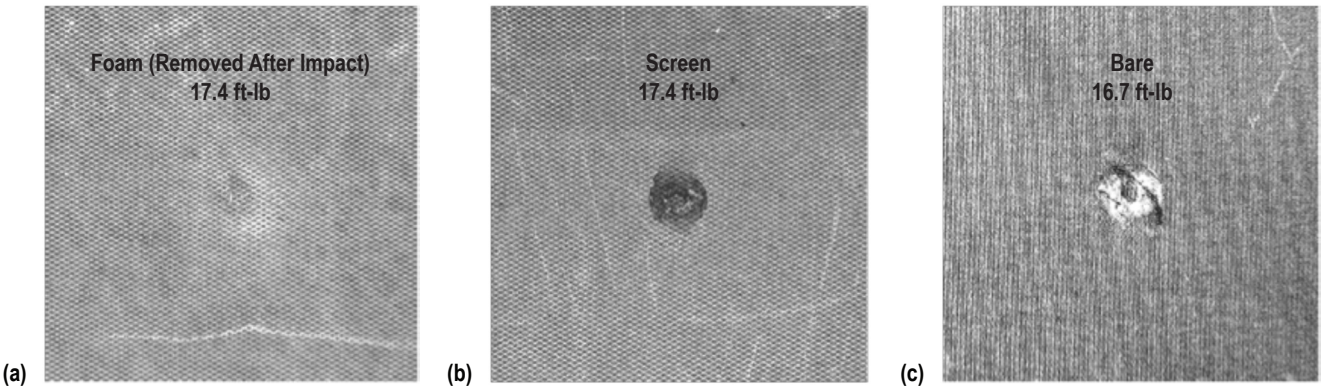

Figure 9. Visual damage on specimens impacted at high-impact levels: (a) Foam, (b) screen, and (c) bare.

Although the foam acts as a good impact indicator, once the foam is removed, the impact event is less visible on the laminates covered with foam than on the screen or bare laminates. Therefore, if there is some type of removable foam covering the laminate, care must be taken to examine the foam for impacts before removal since the foam tends to obscure the visual damage once removed.

4.3 Cross-Sectional Examination

Impacted specimens were cross-sectioned to assess the damage morphology and to better identify what the IRT results are indicating. Typical results for a low-impact level are shown in figure 10. In these images, only one-half of the total cross-sectional damage area is shown since the damage morphology is such that the damage is approximately symmetrical on either half of the impact location. The dimpling or waviness in the plies closest to the core is typical of cocured sandwich structures with a honeycomb core and laminated face sheet.

Obvious differences in the damage morphology could not be determined with certainty at low-impact energies. All specimens impacted at energies below about 8 ft-lb showed approximately the same level of delamination and matrix cracking. The foam did delay the onset of when a delamination was formed; however, once a delamination was formed, it differed little from the bare and screen specimens until about 10 ft-lb of impact energy.

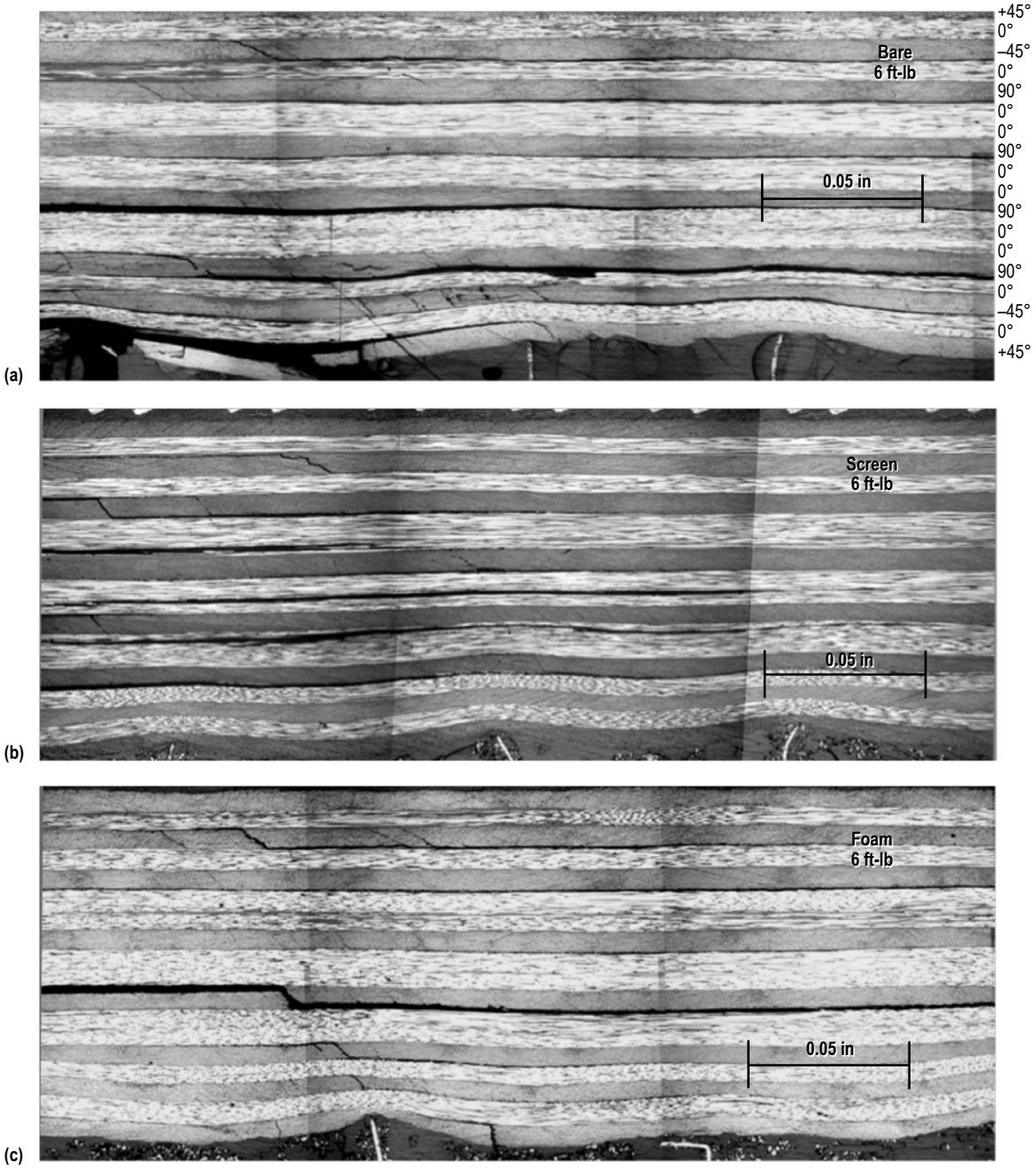

Figure 10. Typical cross sections through the impact zone of specimens impacted with low energy: (a) Bare, (b) screen, and (c) foam.

Typical results for a high-impact level are shown in figure 11. The bare specimen shows fiber breakage in the 0° ply closest to the core. This ply is assumed to carry less load than the central and outer 0° plies due to its waviness from the cocure process. Wavy 0° plies have been shown to reduce the compression strength of a laminate by the proportion of 0° wavy plies to 0° straight plies.[13] Therefore, the emphasis is on the straighter 0° plies away from the core that carry the majority of the compressive load. At high-impact energy, it was noted that the delaminations within the foam specimens tended to be longer than the delaminations on the bare and screen specimens that can be seen by the NDE data in figure 6, which shows a more elliptical shape with the longer axis in the 0° direction. The bare specimens tended to exhibit more damage on the plies closest to the core and on the non-0° plies at the top of the laminate.

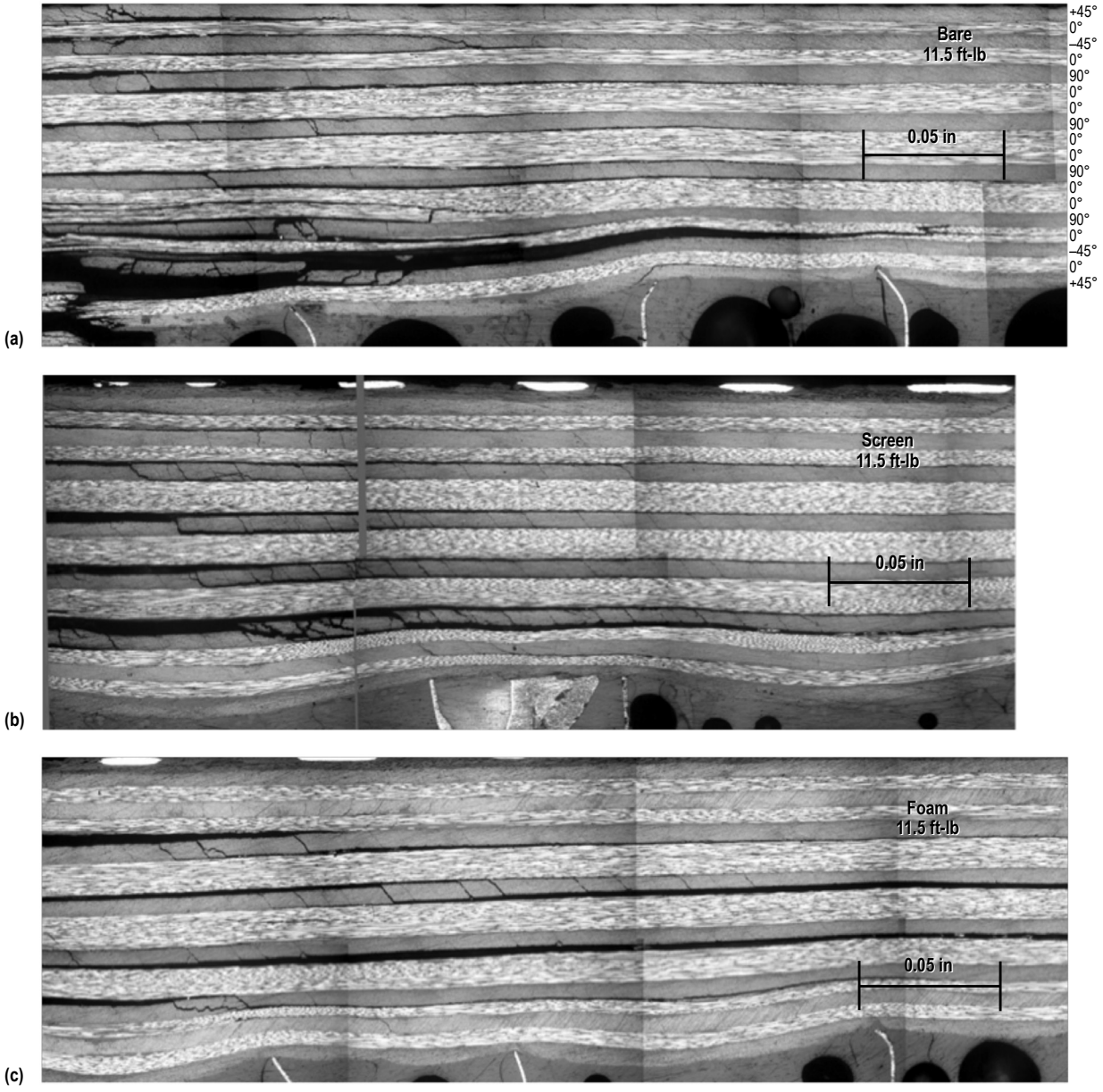

Figure 11. Typical cross sections through the impact zone of specimens impacted with high energy: (a) Bare, (b) screen, and (c) foam.

4.4 Residual Compression Strength

The results from CAI testing of the specimens are plotted in figure 12. Table 2 contains the data that was tabulated.

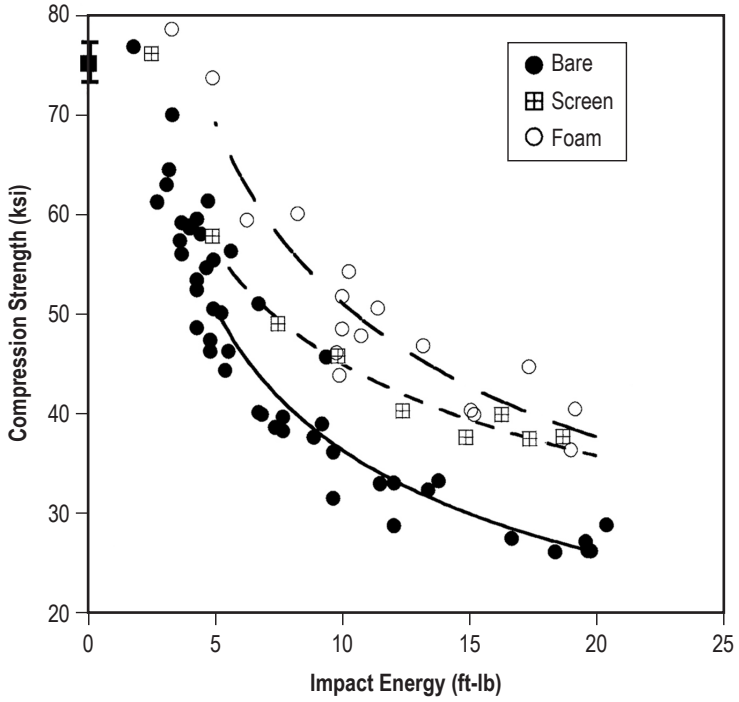

Figure 12. CAI strength versus impact energy results from table 2.

Specimens covered with foam have a higher CAI strength for any given impact energy level. The screen-covered specimens also demonstrate a higher CAI strength than the bare specimens, though not quite to the extent of the foam-covered specimens. Specimens impacted at the lowest energy levels had the same compression strength as undamaged specimens.

At low-impact energies, the screen has CAI strength close to that of the bare specimens, but the screen has about the same CAI strength as the foam specimens at higher impact energies. The importance of testing replicates is highlighted by the large variation in strength.

Table 2. Results of CAI testing.

Bare Specimen I.D.	Impact Energy (ft-lb)	CAI Strength (ksi)	Screen Specimen I.D.	Impact Energy (ft-lb)	CAI Strength (ksi)	Foam Specimen I.D.	Impact Energy (ft-lb)	CAI Strength (ksi)
Bare-1	4.3	52.3	Screen-1	18.7	37.7	Foam-1	11.4	50.5
Bare-2	4.3	48.5	Screen-2	17.4	37.5	Foam-2	3.3	78.4
Bare-3	4.8	46.2	Screen-3	16.3	39.9	Foam-4	4.9	73.5
Bare-4	4.8	47.3	Screen-4	14.9	37.6	Foam-5	6.3	59.3
Bare-5	5.5	46.2	Screen-5	12.4	40.2	Foam-7	15.1	40.3
Bare-6	5.4	44.3	Screen-6	9.9	45.7	Foam-8	9.9	43.8
Bare-7	13.4	32.3	Screen-7	7.5	48.9	Foam-9	10.0	51.6
Bare-8	13.8	33.2	Screen-8	4.9	57.7	Foam-10	10.0	48.4
Bare-9	9.7	36.1	Screen-9	2.4	75.9	Foam-11	8.26	59.9
Bare-10	11.5	32.9				Foam-13	10.3	54.1
Bare-11	12.1	33.0				Foam-14	10.7	47.7
Bare-12	8.9	37.6				Foam-15	9.8	46.0
Bare-13	7.4	38.6				Foam-16	13.2	46.7
Bare-14	6.9	39.9				Foam-17	17.4	44.7
Bare-16	1.8	76.6				Foam-18	19.0	36.4
Bare-19	2.7	61.1				Foam-19	19.2	40.5
Bare-20	4.3	59.4				Foam-20	15.2	39.9
Bare-21	6.7	50.9						
Bare-22	6.7	40.1						
Bare-26	9.7	31.5						
Bare-27	12.0	28.7						
Bare-28	16.7	27.5						
Bare-29	20.4	28.9						
Bare-30	19.6	26.3						
Bare-31	19.6	26.3						
Bare-32	19.6	27.2						
Bare-33	18.4	26.2						
Bare-34	7.7	39.6						
Bare-35	7.7	38.2						
Bare-36	9.2	38.9						
Bare-37	9.4	45.6						
Bare-38	4.4	57.9						
Bare-39	4.7	61.2						
Bare-40	4.9	55.3						
Bare-41	5.6	56.2						
Bare-42	3.6	57.2						
Bare-43	4.1	58.6						
Bare-44	4.3	53.3						
Bare-45	4.6	54.5						
Bare-46	4.9	50.4						
Bare-47	5.2	50.0						
Bare-48	3.1	62.8						
Bare-49	3.3	69.8						
Bare-50	3.2	64.3						
Bare-51	3.7	59.0						
Bare-52	3.7	55.9						
Bare-53	4.0	58.5						
Bare-54	4.0	58.7						

The CAI strength data versus damage width is plotted in figure 13. The undamaged compression strength of 75.8 ksi was not lowered on impacted panels that showed no damage as detected by IRT. Therefore, it is likely that any detrimental damage was detected by NDE.

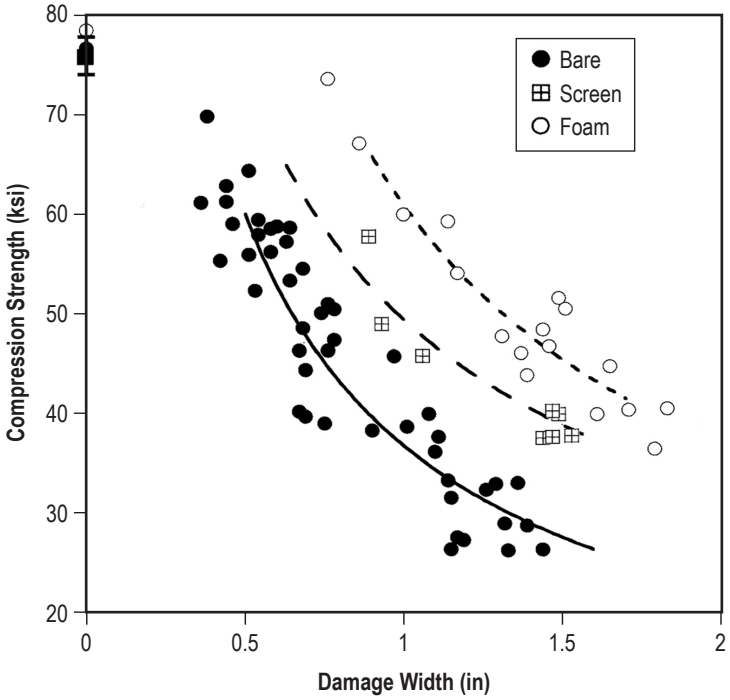

Figure 13. CAI strength versus damage width.

5. DISCUSSION

From the CAI results shown in figure 12, it is apparent that the specimens covered with foam had a higher CAI strength for a given impact energy, which may seem intuitive. However, the damage sizes for the foam specimens were the same or larger than the bare and screen specimens for a given impact energy. Figure 4 illustrates that the foam actually does not 'protect' the specimen from damage. Furthermore, a larger damage size is noted even though the CAI strength for a given size is larger for the foam specimens. This is also illustrated in figure 4 when the foam can appear to be more detrimental to the damage resistance of the laminate at high-impact energies. An alternate explanation of why the damage tolerance of the foam specimens is superior is needed.

This can be explained by the damage morphology of the specimens, as it was in reference 2. A closer examination of the cross sections in figures 10 and 11, with concentration on the outer two 0° plies (since the inner two are wavy and presumably carry much less load), gives some possible explanations for the CAI results.

For specimens impacted at lower impact energies, it was noted that the angle of the matrix crack in the –45° ply below the outermost 0° ply differed between the three types of specimens tested. Figure 14 shows more detailed images of the cross sections shown in figure 10. In general, the bare specimens had larger crack angles when the angle was measured between the crack and the through thickness direction. Figure 14 shows the approximate angle measurements for the specimens examined in figure 10.

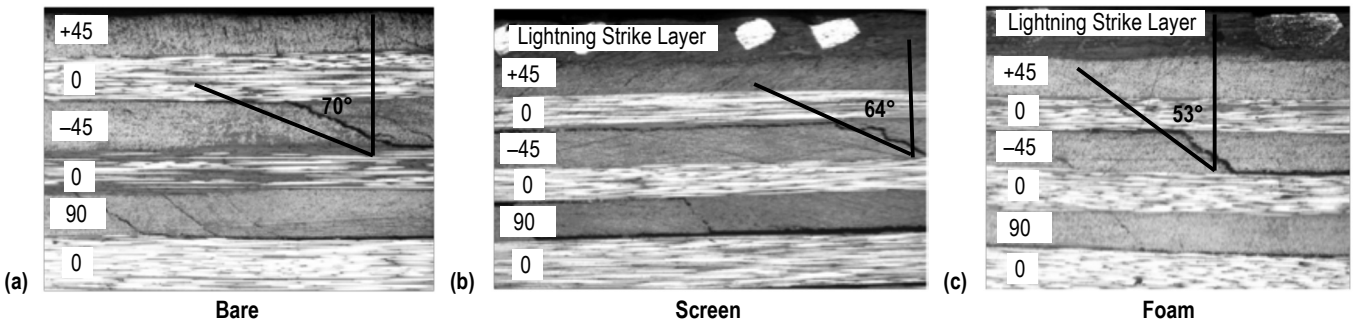

Figure 14. Detail of matrix crack in –45° ply beneath the outmost 0° ply at impact energies below approximately 8 ft-lb for (a) bare, (b) screen, and (c) foam specimens.

It is possible that as the specimen is loaded in compression, the crack has a 'wedge like' effect and causes out-of-plane forces on the neighboring plies. This wedge effect has been explained by Puck and Schurmann and termed 'Mode C Inter-Fiber Failure (IFF).'[14,15] Figure 15 is a two-dimensional representation of this type of failure.

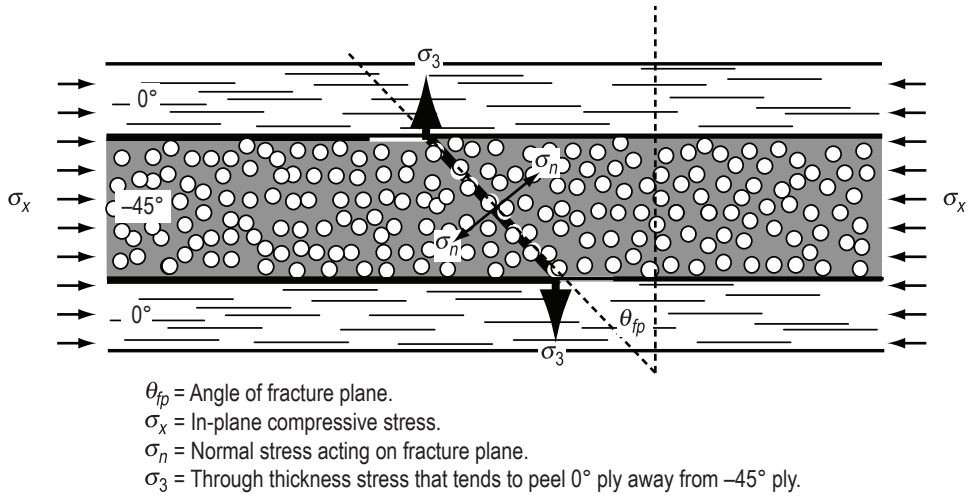

Figure 15. Wedge effect of angled matrix cracks in compression.

As the fracture angle θ_{fp} becomes larger, the in-plane stress σ_x will cause the normal stress σ_n to become larger, which in turn causes the through thickness stress σ_3 to become larger, indicating more likelihood of IFF. The friction between the two inclined planes helps to delay the onset of Mode C IFF; however, once σ_x becomes large enough to overcome this friction, the two halves slide up and over each other causing the neighboring plies to delaminate and become unstable as shown in figure 16.

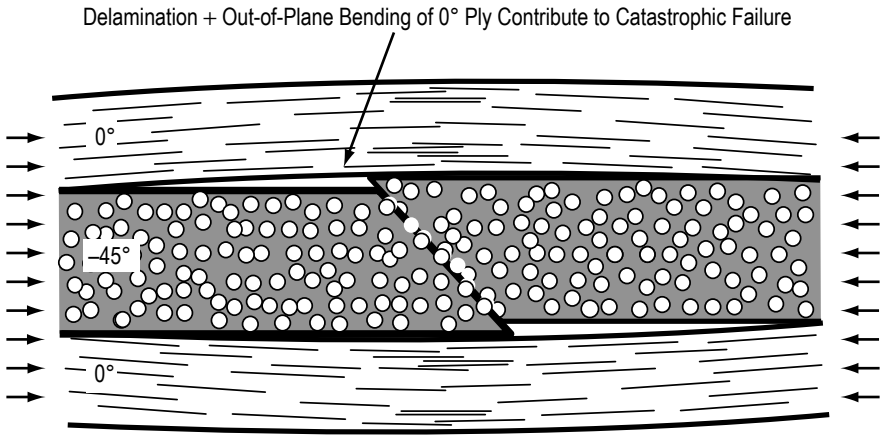

Figure 16. Sliding of wedge sections once the friction between the two is overcome.

It should be noted that the authors of reference 15 demonstrate that in-plane compressive loads typically would not give rise to this type of failure for carbon fiber laminates of the (0°/±45°/90°) family since the 0°-ply failure strain is so much lower than the failure strain needed to cause the inclined matrix cracks needed for the Mode C IFF. However, in this study, the inclined matrix cracks

are caused by an out-of-plane load (impact), and inclined matrix cracks occur due to this type of load as evidence by the cross-sectional photographs in figures 10 and 11.

For specimens impacted at higher impact energies, a closer examination revealed that the plies sandwiching the outermost 0° ply were consistently more heavily damaged in the bare specimens. Overall, the screen specimens tended to have less damage and the foam specimens had practically no damage in these plies. Closer views from figure 11 are shown in figure 17.

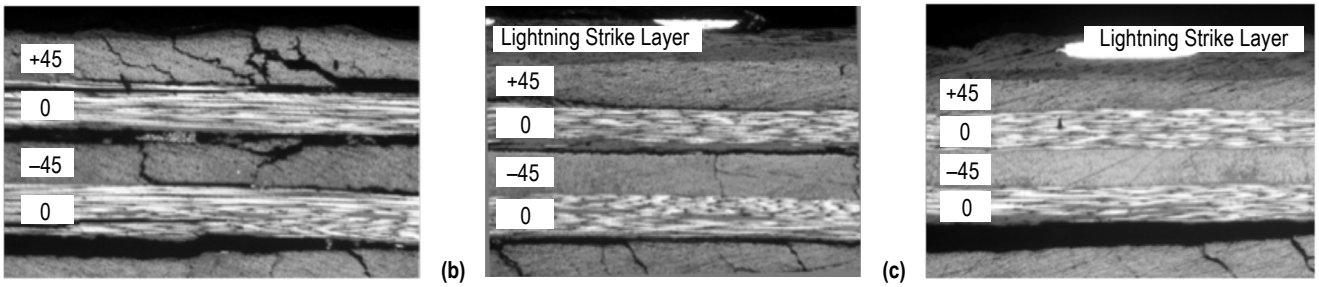

Figure 17. Detail of damage to the +45° and –45° plies sandwiching the outermost 0° ply at impact energy levels above 10 ft-lb for (a) bare, (b) screen, and (c) foam specimens.

Berbinau et al. have shown that the stiffness of plies neighboring the main load carrying 0° plies can have an effect on the compression strength of the laminate and the strength can be reduced by about 20% for laminates composed of 50% 0° plies if an outer ply is a 0° ply.[16] This is shown to be due to out-of-plane microbuckling since one side has no neighboring plies to support the outer 0° ply and force in-plane microbuckling, which is a higher strain-failure event.

Qualitatively, for the outermost 0° ply in the specimens tested at higher impact energies in this study, it can be seen that the bare specimens had the least support from the ±45° plies neighboring them. These specimens typically demonstrated complete delamination at both interfaces along with severe matrix cracking. The screen specimens typically had delamination between both interfaces, but matrix cracking was minimal in the ±45° plies. The foam specimens typically showed no delamination between the interfaces and little to no matrix cracking. Figure 13 shows that for large damage sizes (in the 1.5-in range), the foam specimens had 64% higher compression strength and the screen specimens had 39% higher compression strength than the bare specimens. Thus, when undamaged specimens are compression tested, the lightning strike layer adds negligible stability to the outermost 0° ply but causes a higher CAI strength by preventing the two outer 45° plies from sustaining greater damage. For the foam specimens, the lightning strike layer plus the foam prevent the outer two 45° plies from delaminating from the 0° ply between them.

6. CONCLUSIONS

Although the foam and screen specimens had larger damage sizes based on NDE indications, their residual strength was greater than the bare specimens. This is explained by the different damage morphology that forms.

A difference in damage size for a given impact energy was not evident until about 10 ft-lb, at which point the presence of the foam enabled the occurance of the largest damage, followed by the screen, and then the bare.

The findings in this study were similar to those found in reference 2 for high-strength fiber, namely that TPS causes a different damage morphology, which leads to the different CAI results.

No loss in strength was seen for panels that did not exhibit damage as detected by flash thermography NDE techniques. The flash thermography NDE technique detected all detrimental damage seen in this study.

The foam-covered specimens require larger minimum impact energy to form damage, and, once it forms, the smallest damage size is larger than the bare or screen specimens impacted at the same levels. The threshold of impact energy required to create damage detectable by IRT was increased by 79% for the foam coating.

At higher impact energies, the lightning strike layer protects the outermost ±45° plies. With less damage in the outermost ±45° plies, the outermost 0° ply is more stabilized than in the bare composites that exhibited greater damage in the ±45° plies.

At the lower end of impact energies examined in this study, the higher CAI strength for the foam-covered specimens can be explained by Mode C IFF as outlined by Puck in references 14 and 15.

At the higher end of impact energies examined in this study, the higher CAI strength for the foam and screen specimens can be explained by improved stability of the outermost 0° ply.

The most significant aspect of having TPS foam and a lightning strike layer is that these layers act as good impact indicators as well as protection. This comes at a cost of a 6.9% increase in mass (areal weight). Impacts in the foam coating were clearly visible at 2.2 ft-lb of impact energy while the screen specimens did not exhibit barely visible damage until 12.4 ft-lb, and the bare specimens exhibited BVID at 8.5 ft-lb.

REFERENCES

1. "Fracture Control Requirements for Composite and Bonded Vehicle and Payload Structures," *MSFC–RQMT–3479*, Marshall Space Flight Center, AL, June, 2006.

2. Petit, S.; Bouvet, C.; Bergerot, A.; and Barrau, J-J.: "Impact and Compression After Impact Experimental Study of a Composite Laminate With a Cork Thermal Shield," *Compos. Sci. Technol.*, Vol. 67, Nos. 15–16, pp. 3286–3299, 2007.

3. Adams, D.F.; and Zimmerman, R.S.: "Static and Impact Performance of Polyethylene Fibe-Graphite Fiber Hybrid Composites," *SAMPE J.*, Vol. 22, No 6, pp. 10–16, 1986.

4. Busgen, A.W.; Effing, M.; and Scholle, M.: "Improved Damage Tolerance of Carbon Fiber Composites by Hybridization With Polyethylene Fiber, Dyneema SK 60," *Proc. American Society for Composites Fourth Technical Conference*, pp. 418–423, 1989.

5. Peijs, A.A.J.M.; Venderbosch, R.W.; and Lemstra, P.J.: " Hybrid Composites Based on Polyethylene and Carbon Fibers Part 3: Impact Resistant Structural Composites Through Damage Management," *Compos. Eng.*, Vol. 21, No. 6, pp. 522–530, 1990.

6. Nettles, A.T.; and Lance, D.G.: "On the Enhancement of Impact Damage Tolerance of Composite Laminates," *Compos. Eng.*, Vol. 3, No. 5, pp. 383–394, 1993.

7. Shuart, M.J.; Prasad, C.B.; and Biggers, S.B.: "A Protection and Detection Surface (PADS) for Damage Tolerance," *NASA TP—3011*, Langley Research Center, Hampton, VA, 1990.

8. Hart, W.G.J.; and Ubels, L.C.: "Impact Energy Absorbing Surface Layers for Protection of Composite Aircraft Structures," *NLR–TP–98002,* National Aerospace Laboratory NLR, Amsterdam, The Netherlands, 1998.

9. *Application Guide-Specialty Applications, Composite Protection*, Mask-Off Company, Inc., Monrovia, CA, 2007.

10. *Aircraft Flight Surface Protection Solution*, 3M Aerospace and Aircraft Maintenance Division, St. Paul, MN, 2005.

11. Nettles, A.T.; and Jackson, J.R.: "Compression After Impact Testing of Sandwich Composites for Usage on Expendable Launch Vehicles," *J. Compos. Mater.*, Vol. 44, No. 6, pp. 707–738, 2010.

12. Lee, S.M.; and Zahuta, P.: "Instrumented Impact and Static Indentation of Composites," *J. Compos. Mater.*, Vol. 25, No. 2, pp. 204–222, 1991.

13. Adams, D.O.; and Bell, S.J.: "Compression Strength Reductions in Composite Laminates Due to Multiple-Layer Waviness," *Compos. Sci. Technol.*, Vol. 53, No. 2, pp. 207–212, 1995.

14. Puck, A.; and Schurmann, H.: "Failure Analysis of FRP Laminates by Means of Physically Based Phenomenological Models," *Compos. Sci. Technol.*, Vol. 62, Nos. 12–13, pp. 1633–1662, 2002.

15. Puck, A.; and Schurmann, H.: "Failure Analysis of FRP Laminates by Means of Physically Based Phenomenological Models," *Compos. Sci. Technol.*, Vol. 58, No. 7, pp. 1045–1067, 1998.

16. Berbinau, P.; Soutis, C.; Goutas, P.; and Curtis, P.T.: "Effect of Off-Axis Ply Orientation on 0°-Fibre Microbuckling," *Compos. Part A: Appl. S.*, Vol. 30, No. 10, pp. 1197–1207, 1999.

REPORT DOCUMENTATION PAGE

Form Approved
OMB No. 0704-0188

PLEASE DO NOT RETURN YOUR FORM TO THE ABOVE ADDRESS.

1. REPORT DATE *(DD-MM-YYYY)*	2. REPORT TYPE	3. DATES COVERED *(From - To)*
01–02–2011	Technical Publication	

4. TITLE AND SUBTITLE

The Effects of Foam Thermal Protection System on the Damage Tolerance Characteristics of Composite Sandwich Structures for Launch Vehicles

5a. CONTRACT NUMBER

5b. GRANT NUMBER

5c. PROGRAM ELEMENT NUMBER

6. AUTHOR(S)

A.T. Nettles, A.J. Hodge, and J.R. Jackson

5d. PROJECT NUMBER

5e. TASK NUMBER

5f. WORK UNIT NUMBER

7. PERFORMING ORGANIZATION NAME(S) AND ADDRESS(ES)

George C. Marshall Space Flight Center
Marshall Space Flight Center, AL 35812

8. PERFORMING ORGANIZATION REPORT NUMBER

M–1306

9. SPONSORING/MONITORING AGENCY NAME(S) AND ADDRESS(ES)

National Aeronautics and Space Administration
Washington, DC 20546–0001

10. SPONSORING/MONITOR'S ACRONYM(S)

NASA

11. SPONSORING/MONITORING REPORT NUMBER

NASA/TP—2011–216457

12. DISTRIBUTION/AVAILABILITY STATEMENT

Unclassified-Unlimited
Subject Category 24
Availability: NASA CASI (443–757–5802)

13. SUPPLEMENTARY NOTES

Prepared by the Materials Processes and Manufacturing Department, Engineering Directorate

14. ABSTRACT

For any structure composed of laminated composite materials, impact damage is one of the greatest risks and therefore most widely tested responses. Typically, impact damage testing and analysis assumes that a solid object comes into contact with the bare surface of the laminate (the outer ply). However, most launch vehicle structures will have a thermal protection system (TPS) covering the structure for the majority of its life. Thus, the impact response of the material with the TPS covering is the impact scenario of interest. In this study, laminates representative of the composite interstage structure for the Ares I launch vehicle were impact tested with and without the planned TPS covering, which consists of polyurethane foam. Response variables examined include maximum load of impact, damage size as detected by nondestructive evaluation techniques, and damage morphology and compression after impact strength. Results show that there is little difference between TPS covered and bare specimens, except the residual strength data is higher for TPS covered specimens.

15. SUBJECT TERMS

damage tolerance, sandwich, launch vehicle, compression after impact, thermal protection

16. SECURITY CLASSIFICATION OF:			17. LIMITATION OF ABSTRACT	18. NUMBER OF PAGES	19a. NAME OF RESPONSIBLE PERSON
a. REPORT	b. ABSTRACT	c. THIS PAGE			STI Help Desk at email: help@sti.nasa.gov
U	U	U	UU	32	19b. TELEPHONE NUMBER *(Include area code)* STI Help Desk at: 443–757–5802

National Aeronautics and
Space Administration
IS20
George C. Marshall Space Flight Center
Marshall Space Flight Center, Alabama
35812